

**Synthesis and Characterization of La doped**

**BaTiO<sub>3</sub> ceramic By sol-gel route**

**A Dissertation Submitted in partial fulfilment**

**FOR THE DEGREE OF MASTER OF SCIENCE IN PHYSICS**

**Under Academic Autonomy**

**NATIONAL INSTITUTE OF TECHNOLOGY, ROURKELA**

**By**

**ARPITA MISHRA**

**Under the Supervision of**

**Prof. S. Panigrahi**



**DEPARTMENT OF PHYSICS**

**NATIONAL INSTITUTE OF TECHNOLOGY**

**ROURKELA – 769008**



**NATIONAL INSTITUTE OF TECHNOLOGY**

**ROURKELA**

**CERTIFICATE**

This is to certify that the thesis entitled, **“Synthesis and Characterization of La doped BaTiO<sub>3</sub>”** submitted by Miss. Arpita Mishra in partial fulfilments for the requirements for the award of Master of Science Degree in Physics Department at National Institute of Technology, Rourkela is an authentic work carried out by him under my supervision and guidance.

To the best of my knowledge, the matter embodied in the project has not been submitted to any other University/ Institute for the award of any Degree or Diploma.

Rourkela-769008

Prof.S.Panigrahi

Date:

Dept. of Physics

National Institute of Technology

# ACKNOWLEDGEMENT

With deep regards and profound respect, I avail this opportunity to express my deep sense of gratitude and indebtedness to Prof. S. Panigrahi, Department of Physics, National Institute of Technology Rourkela, for introducing the present project topic and for his inspiring guidance, constructive criticism and valuable suggestion throughout the project work. I most gratefully acknowledge his constant encouragement and help in different ways to complete this project successfully.

I would like to acknowledge my deep sense of gratitude to Prof.S. Jena, Head, Department of Physics, National Institute of Technology Rourkela, for his valuable advices and constant encouragement for allowing me to use the facilities in the laboratory.

I wish to thank all the faculty members & staffs of Department of Physics for their support and help during the project.

It give me great pleasure to express my heartfelt gratitude to the laboratory mate Mr. Senthil.V who have made it so easy to work in the laboratory by providing me with an utmost friendly humorous and amicable atmosphere to work in.

Last but not the least; I would like to express my gratefulness to my parents for their endless support, without which I could not complete my project work. I would also like to thanks to my friends and all the Ph.D. students in our physics department for their valuable help.

Rourkela

Arpita Mishra

Date:

## CONTENTS

	Page No.
ABSTRACT	
CHAPTER 1 INTRODUCTION	1
1.1 Ferroelectric Material	2
1.2 Ferroelectric domain	3
1.3 Barium titanate	7
1.4 Application of ferroelectric materials	9
CHAPTER-2 MOTIVATION	12
CHAPTER-3 THESIS OBJECTIVE	13

## CHAPTER-4 EXPERIMENTAL TECHNIQUE

4.1 Synthesis methods	14
-----------------------	----

4.2 Experimental work	17
-----------------------	----

## CHAPTER-5 RESULTS AND DISCUSSION

5.1 XRD Analysis	19
------------------	----

5.2 SEM analysis	22
------------------	----

5.3 DSC and TG analysis	24
-------------------------	----

5.4 Dielectric	25
----------------	----

5.5 P-E Loop Measurement	27
--------------------------	----

CHAPTER-6 CONCLUSIONS	29
-----------------------	----

## REFERENCES

## ABSTRACT

Polycrystalline La doped BaTiO<sub>3</sub> (BT) ceramic with general formula Ba<sub>1-x</sub>La<sub>2x/3</sub>TiO<sub>3</sub> (x = 0, 0.01, 0.025, 0.05, 0.075, 0.1) ceramics were prepared by Sol gel route. The DSC-TGA graph shows that the organic materials are getting removed at the time of endothermic reaction and getting crystallized at the time of exothermic reaction. Structural property of all compositions is studied by XRD .The well-defined XRD pattern was observed which shows single phase with tetragonal structure. From XRD graph, it is also seen that the peak is shifting towards right with increase in La concentration in the composition. Surface morphology of the pellets sintered by microwave furnace is studied by SEM analysis. SEM images show that with increase in doping concentration the grain size decreases. The temperature and frequency dependency dielectric study of BaTiO<sub>3</sub> composition sintered at 12500C for 20 mins. is studied. Curie constant values are calculated from the Curie Weiss law.

## CHAPTER-1

### INTRODUCTION

BaTiO<sub>3</sub> is the most widely used ferroelectric material, and even sixty years after its discovery, it is the most important multilayer ceramic dielectric. The objective of this short paper is to indicate some of the chronologically important scientific contributions enhancing the understanding and use of BaTiO<sub>3</sub>. BaTiO<sub>3</sub> was discovered during World War II in 1941 and 1944 in the United States, Russia, and Japan. At least in the U.S.A., the research was accelerated because of the war. At that time, mica was used in most capacitors, but U-boats threatened the supplies of mica to the U.S.A. from South America. The initial reports were based on doping studies of TiO<sub>2</sub> with BaO, which produced ceramic materials with enhanced dielectric permittivities.

---

When an electric field is applied to an ideal dielectric material, there is no long-range transport of charge but only a limited rearrangement of charges such that the dielectric acquires a dipole moment and is said to be polarized. Atomic polarization, which occurs in all materials, is a small displacement of the electrons in an atom relative to the nucleus. In ionic materials there is, in addition, ionic polarization involving the relative displacement of cation and anion sublattices. Dipolar materials, such as water, can become polarized because the applied electric field orients the molecules. Finally, space charge polarization involves a limited transport of charge carriers until they are stopped at a potential barrier, possibly a grain boundary or phase boundary. An individual atom or ion in a dielectric is not subjected directly to an applied field but to a local field which has a very different value and under certain conditions, lattice polarization produces a local field which tends to stabilize the polarization further – a feedback mechanism. This points to the possibility of “spontaneous polarization” i.e., lattice polarization in the absence of an applied field. Such spontaneously polarized materials do exist and “ferroelectrics” constitute an important class among them. The two conditions necessary in a material to classify it as a ferroelectric are (1) the existence of spontaneous polarization and (2) a demonstrated reorientation of the polarization by an applied electric field. Spontaneous polarization is

defined as a stable polarization of a crystal in the absence of an external electric field. The spontaneous polarization changes with temperature. There is a critical point—known as the Curie temperature—that defines the transition to a spontaneous polarization state from a state that is originally electrically neutral. Above the Curie temperature, the crystal is electrically neutral and its crystallographic phase is called paraelectric; below the Curie temperature, the crystal is spontaneously polarized and this crystallographic phase is called ferroelectric.

## 1.1 FERROELECTRIC MATERIALS

Polar materials possess an effective electric dipole moment in the absence of an external field. In general, the individual dipoles are randomly oriented in the space. In so-called pyroelectric materials, all dipoles are oriented in the same sense, creating surface charge, which is a measure of the macroscopic spontaneous polarization,  $P_s$ . Ferroelectrics are a special case of polar materials where spontaneous polarization  $P_s$  possesses at least two equilibrium states; the direction of the spontaneous polarization vector may be switched between those orientations by an electric field. The crystal symmetry requires that all ferroelectric materials must be pyroelectric and all pyroelectric materials must be piezoelectric. Today, the majority of piezoelectric materials in practical use, with the important exception of quartz, are ferroelectrics. The modern definition of ferroelectric polarization can be found in some recent texts, but for our purposes we can limit ourselves to the simple approach given here. Most ferroelectric materials undergo a structural phase transition from a high-temperature nonferroelectric (or paraelectric) phase into a low-temperature ferroelectric phase. Some ferroelectrics, like barium titanate, **BaTiO<sub>3</sub>**, undergo several phase transitions into successive ferroelectric phases. The transition into a ferroelectric phase usually leads to strong anomalies in the dielectric, elastic, thermal and other properties of the material and is accompanied by changes in the dimensions of the crystal unit cell. The associated strain is called the spontaneous strain,  $X_s$ .



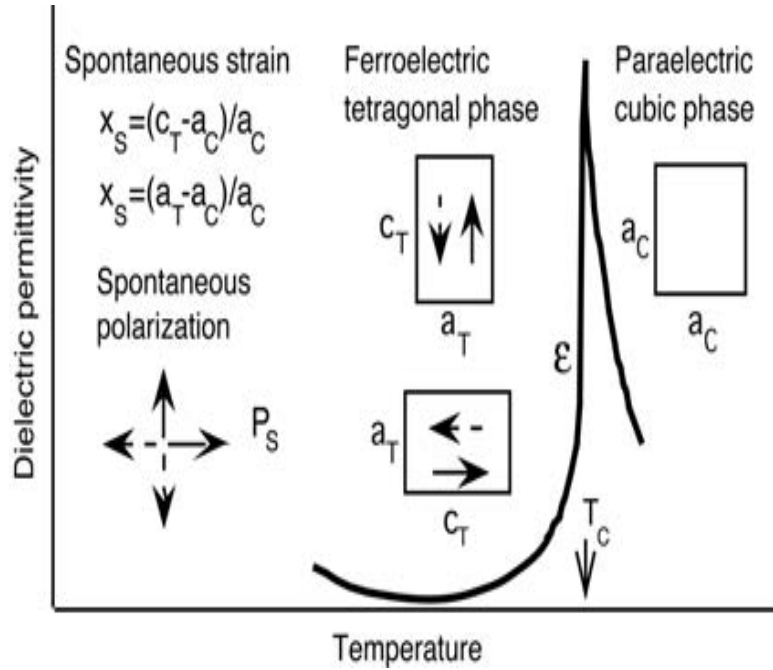


**FIGURE 1.** Illustration of the changes in a two-axial ferroelectric material as it transform from a paraelectric cubic into a ferroelectric tetragonal state.

It represents the relative difference in the dimensions of the ferroelectric and paraelectric unit cells. Some changes that can occur in a ferroelectric material that transforms from a paraelectric cubic into a ferroelectric tetragonal phase are illustrated in Fig.1

## 1.2 FERROELECTRIC DOMAINS

To introduce ferroelectric domains, and avoid a too general discussion, we take as an example lead titanate,  $\text{PbTiO}_3$ . Lead titanate is a perovskite crystal that transforms from a nonferroelectric cubic to a ferroelectric tetragonal phase at  $490^\circ \text{C}$ . Perovskite crystals have a general formula  $\text{ABO}_3$ , where valence of A cations takes values from +1 to +3 and of B cations from +3 to +6. As shown in Fig.2, the structure may be viewed as consisting of  $\text{BO}_6$  octahedra surrounded by A cations. Most of the ferroelectric materials that are of practical interest have a perovskite structure and many, such as lead zirconate titanate,  $\text{Pb}(\text{Zr,Ti})\text{O}_3$ , are solid solutions of  $\text{PbTiO}_3$ . The spontaneous polarization in  $\text{PbTiO}_3$  lies along the  $c_T$ -axis of the tetragonal unit cell and the crystal distortion is usually described in terms of the shifts of O and Ti ions relative to Pb. In the ferroelectric phase, the crystal is spontaneously strained with  $a_T (= 0.390 \text{ nm}) < a_C < c_T (= 0.415 \text{ nm})$ , where  $a_T$  and  $a_C$  are the a-axes of the tetragonal and cubic unit cells, and  $c_T$  is the c-axis of the tetragonal cell. The spontaneous polarization in a ferroelectric crystal (or a grain in a ferroelectric film or ceramic) is usually

not uniformly aligned throughout the material along the same direction. The six directions (including

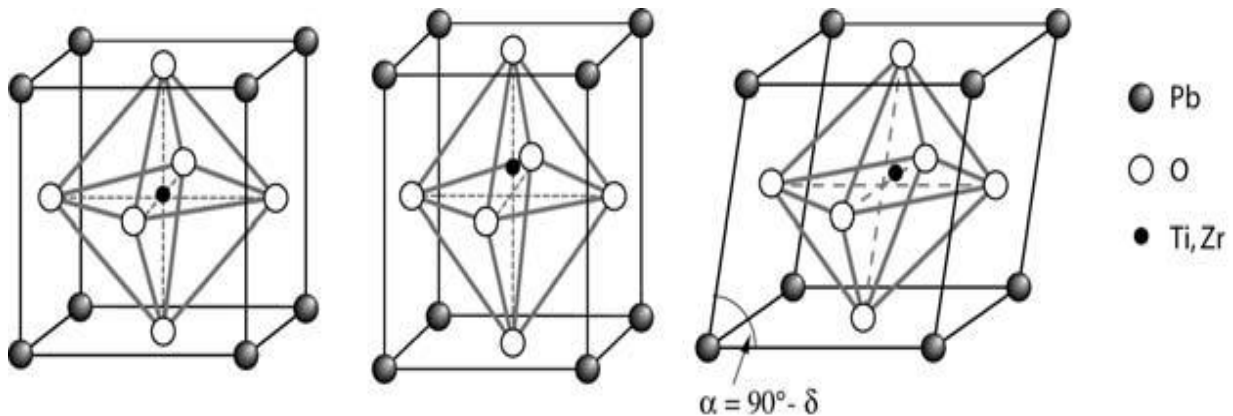


**FIGURE 2.** Perovskite crystal in its paraelectric cubic (left), ferroelectric tetragonal (middle), and rhombohedral (right) states.  $\text{PbTiO}_3$ , which is cubic in the paraelectric phase and tetragonal in the ferroelectric phase, can adopt rhombohedral structure when modified by about 50 per cent Zr.

positive and negative orientations) along the three  $a_C$  -axes of the cubic cell in  $\text{PbTiO}_3$  are equivalent, and spontaneous polarization may arise with equal probability along any of them when the crystal is cooled through the ferroelectric phase-transition temperature. Directions along which the polarization will develop depend on the electrical and mechanical boundary conditions imposed on the sample, as discussed below. The regions of the crystal with uniformly oriented spontaneous polarization are called ferroelectric domains. The region between two domains is called a domain wall. The walls that separate domains with oppositely oriented polarization are called  $180^\circ$  walls and those that separate regions with mutually perpendicular polarization are called  $90^\circ$  walls (Fig. 2). Because  $c_T$  – and  $a_T$  -axes in a tetragonal crystal are different, the angle between polarization directions on each side of a  $90^\circ$  domain wall is slightly smaller than  $90^\circ$ . In the domain-wall region, the polarization changes from one domain to another continuously but steeply. The ferroelectric domain walls are therefore much narrower than the domain walls in ferromagnetic materials. Observations with transition electron microscopy show that the width of the domain walls in ferroelectric materials is of the order of 1-10nm, that is, as little as 2--3 crystal unit cells. The width of the domains increases with increasing temperature, as the phase transition is approached. The ferroelectric domains form to minimize the electrostatic energy of the depolarizing fields and

the elastic energy associated with the mechanical constraints to which the ferroelectric material is subjected as it is cooled through the paraelectric--ferroelectric phase transition .

Onset of spontaneous polarization at the transition temperature leads to the formation of surface charges. This surface charge produces an electric field, called the depolarizing field  $E_d$ , which is oriented oppositely to  $P_s$ .

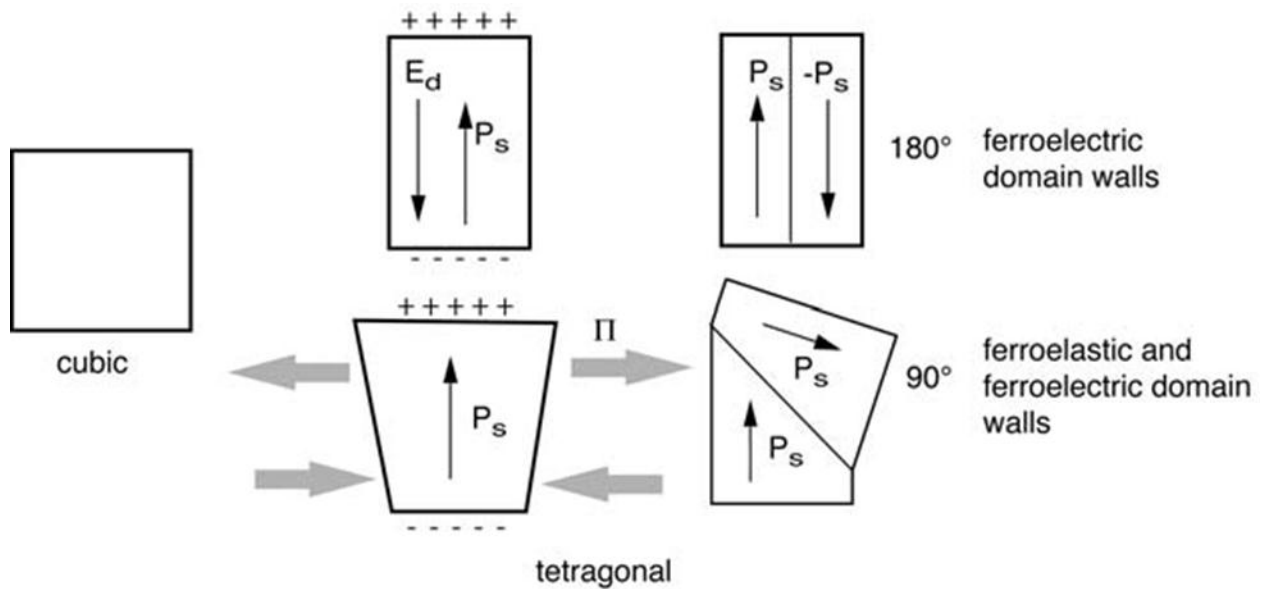


**FIGURE 3.** Illustration of the formation of  $180^\circ$  and  $90^\circ$  ferroelectric domain walls in a tetragonal perovskite ferroelectric. Tetragonal distortion is exaggerated. Effects of the depolarizing field,  $E_d$  and the stresses, are minimized by the creation of domain walls.

The depolarizing field will form whenever there is a non-homogeneous distribution of the spontaneous polarization, for example, due to the fall-off of the polarization near the surface of the ferroelectric (Polarization is zero outside the ferroelectric and nonzero inside) or due to a change in the direction of the polarization at grain boundaries. The depolarizing field may be very strong (of the order of MV/m) rendering the single-domain state of the ferroelectric energetically unfavourable.

The electrostatic energy associated with the depolarizing field may be minimized if:  
 (i) the ferroelectric splits into domains with oppositely oriented polarization, Fig.3, or  
 (ii) the depolarizing charge is compensated by electrical conduction through the crystal or by charges from the surrounding material (for example, from atmosphere or the electric circuit to which the material is connected).

The depolarizing field often cannot be completely compensated, and as grown ferroelectric crystals often exhibit reduced or even zero pyroelectric and piezoelectric effects due to the presence of ferroelectric domains.

Splitting of a ferroelectric crystal into domains may also occur due to the influence of mechanical stresses, as shown in Fig.4. Assume that a part of the  $\text{PbTiO}_3$  crystal is mechanically compressed along the  $[100]$  cubic direction as it is cooled through the phase-transition temperature. To minimize the elastic energy, the long  $c$ -axis of the tetragonal cell will develop perpendicularly to the stress. In the unstressed part of the crystal, the polarization may remain parallel to the direction of the stress (short  $a$ -axis perpendicular to the stress). The domain walls in  $\text{PbTiO}_3$  may therefore separate regions in which polarization orientation is antiparallel ( $180^\circ$  walls) or perpendicular ( $90^\circ$  walls) to each other. Both  $90^\circ$  and  $180^\circ$  walls may reduce the effects of depolarizing electric fields but only formation of  $90^\circ$  walls may minimize the elastic energy. A combination of electrical and elastic boundary conditions to which a crystal is subjected as it is cooled through the ferroelectric phase-transition temperature usually leads to a complex domain structure with many  $90^\circ$  and  $180^\circ$  walls. Since domain walls themselves carry energy, the resulting domain-wall configuration will be such that the sum of the domain-wall energy, crystal surface energy, and elastic and electric fields energy is minimal.

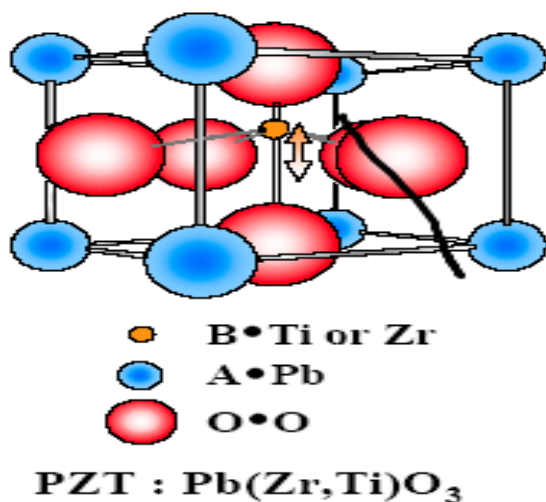
The domain walls that differ in orientation from the spontaneous polarization vector are called ferroelectric domain walls and those that differ in orientation from the spontaneous strain tensor are called ferroelastic domain walls. In  $\text{PbTiO}_3$ , the  $180^\circ$  walls are purely ferroelectric because they differ only in orientation of the polarization vector. The  $90^\circ$  walls are both ferroelectric and ferroelastic, as they differ in orientation of both the polarization vector and the spontaneous strain tensor.

The types of domain walls that can occur in a ferroelectric crystal depend on the symmetry of both nonferroelectric and ferroelectric phases of the crystal. In the rhombohedral phase of the lead zirconate titanate and  $\text{BaTiO}_3$ , for example, the direction of the polarization develops along the body diagonals (direction  $111$ ) of the paraelectric cubic unit cell. This gives eight possible directions of the spontaneous polarization with  $180^\circ$ ,  $71^\circ$  and  $109^\circ$  domain walls.

## 1.3 Barium titanate

BaTiO<sub>3</sub> is the first piezoelectric transducer ceramic ever developed. BaTiO<sub>3</sub> is isostructural with the mineral perovskite (CaTiO<sub>3</sub>) and so is referred to as ‘a perovskite’. Above its Curie point (approximately 130°C) the unit cell is cubic. Below the Curie point the structure is slightly distorted to the tetragonal form with a dipole moment along c direction. Other transformations occur at temperatures close to 0°C and -80°C: below 0°C the unit cell is orthorhombic with the polar axis parallel to a face diagonal and below -80°C, it is rhombohedral with the polar axis along a body diagonal.

[Perovskite Structure]



[D-E Hysteresis Curve]

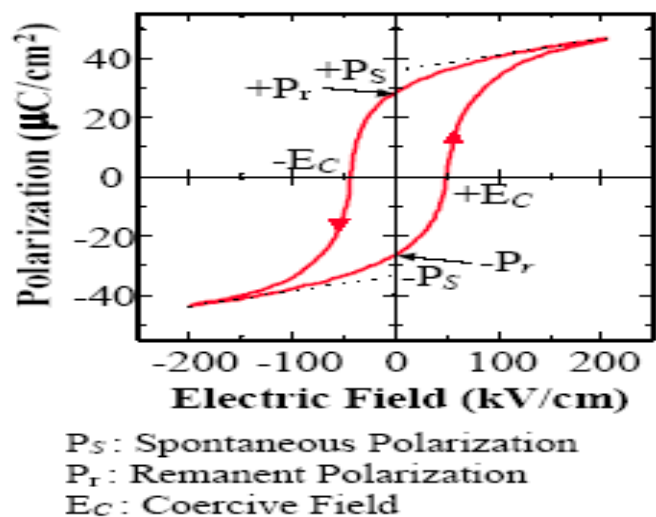


**Fig.4.** Perovskite ABO<sub>3</sub> unit cell for BaTiO<sub>3</sub> illustrating 180° polarization reversal for two of the six possible polarization states produced by displacement of the central cation in the tetragonal plane.

A typical ABO<sub>3</sub> unit-cell structure is given in Fig.4. For example, the BaTiO<sub>3</sub> unit cell consists of a corner-linked network of oxygen octahedra with Ti<sup>4+</sup> ions occupying sites (B sites) within the octahedral cage and the Ba<sup>2+</sup> ions situated in the interstices (A sites) created by the linked octahedra. When an electric field is applied to this unit cell, the Ti<sup>4+</sup> ion moves to a new position along the direction of the applied field. Because the crystallite and hence, the unit cell is randomly oriented and the ions are constrained to move only along certain crystallographic directions of the unit cell, it is most often the case that an individual ionic movement only closely approximates an alignment with the electric field. However, when

this ionic movement does occur, it leads to a macroscopic change in the dimensions of the unit cell and the ceramic as a whole. The dimensional change can be as large as a few tenths of a percent elongation in the direction of the field and approximately one-half of that amount in the other two orthogonal directions. The original random orientation of the domain polarization vectors (virgin condition) can be restored by heating the material above its  $T_c$ . This process is known as thermal depoling.

$\text{BaTiO}_3$  assumes five different crystal structures namely, hexagonal, cubic, tetragonal, orthorhombic, and rhombohedral. The hexagonal and cubic structures are paraelectric while the tetragonal, orthorhombic and the rhombohedral forms are ferroelectric in nature.

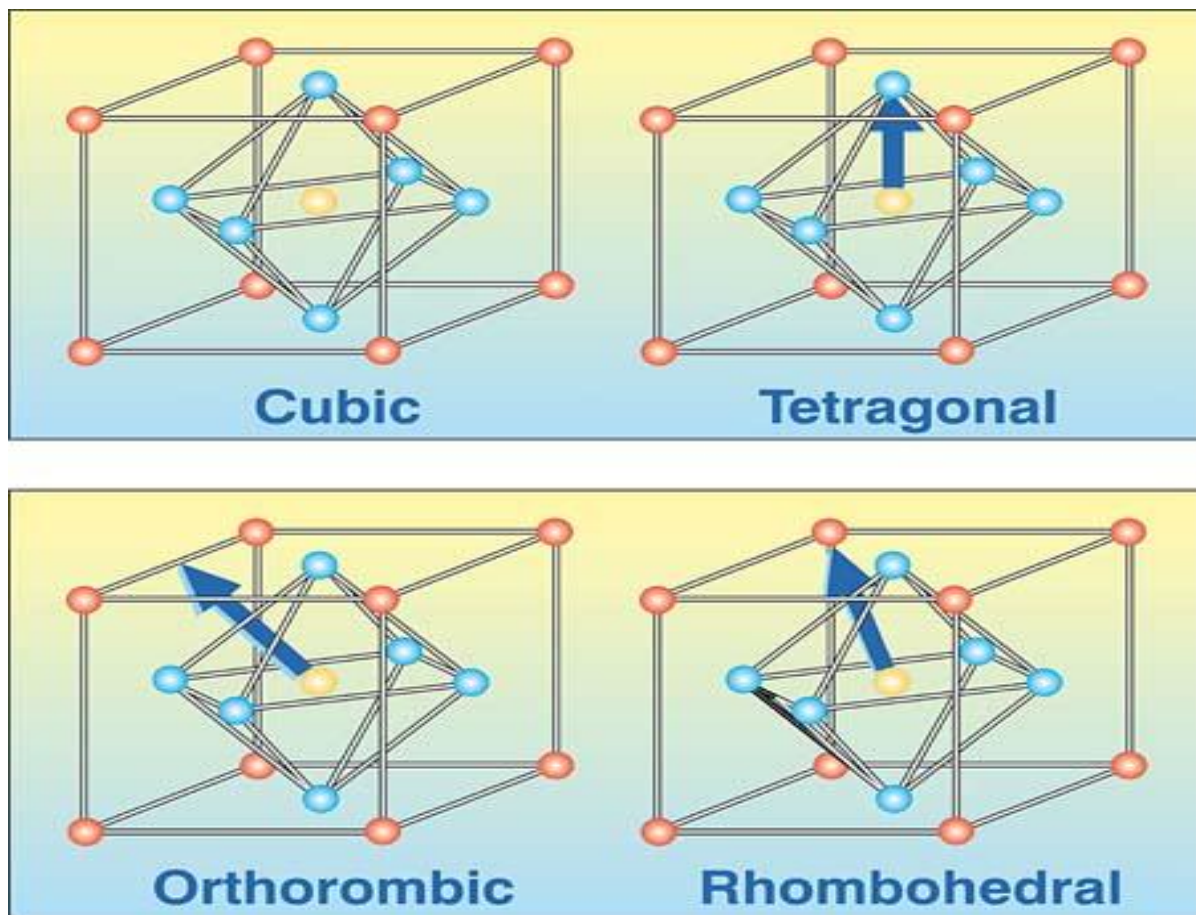


Fig.5. Phase diagram of  $\text{BaTiO}_3$

**Fig.4.** shows hexagonal BaTiO<sub>3</sub> structure is stable above 1460<sup>0</sup>C. Reconstructive hexagonal phase to cubic phase transformation occurs on cooling BaTiO<sub>3</sub> below 1460<sup>0</sup>C. Of utmost important parameter relating to its dielectric application is the ferroelectric - paraelectric transition which occurs at the Curie temperature (around 130<sup>0</sup>C). At this temperature, paraelectric cubic BaTiO<sub>3</sub> transforms into the ferroelectric tetragonal structure following an elongation along an edge. The tetragonal phase is stable until 0<sup>0</sup>C, where it transforms into the orthorhombic phase by elongation along a phase diagonal. Finally, there is a low temperature transition at - 90<sup>0</sup>C where the orthorhombic phase transformed to the rhombohedral phase.

It is used for this application due to its high dielectric constant and low dielectric loss. The values of the dielectric constant depend on the synthesis route, which means purity, density, grain size.

## 1.4 Application of Ferroelectric materials

The applications for ferroelectric ceramics are manifold and pervasive, covering all areas of our workplaces, homes, and automobiles. Similar to most materials, the successful applications of piezoelectric, pyroelectric, ferroelectric, electrostrictive, and electro optic ceramics and films are highly dependent on the relative ease with which they can be adapted to useful and reliable devices.

One category of applications for ferroelectric materials is that of high-dielectric-constant capacitors, particularly *Multilayer capacitor* (MLCs). MLCs are extremely important to our everyday lives in that they are essential to all of our currently produced electronic components, and, as such, they constitute a significant portion of the multibillion dollar electronic ceramics business as a whole. Typical applications include general-use discrete capacitors and MLCs, voltage-variable capacitors, and energy-storage capacitors. Another application of ferroelectric material is BaTiO<sub>3</sub> based PTC ceramic possessing electrically conducting properties at room temperature and rather abruptly changing to a highly resistive material at some elevated temperature at  $T_c$ . Applications include switches, sensors, motor starter and controller .

Ferroelectric materials found applications in *electro optics and photonics* due to their change in optical properties and ferroelectric polarization with an applied electric field. PLZT shutter and linear gate arrays found applications in flash goggles, cockpit viewing port,

offset image setter, film writer and premier image enhancement systems. LiNbO<sub>3</sub> crystal is transparent from the band gap edge absorption at about 320 nm (~3.9 eV) up to the first infrared vibrational absorptions at a wavelength of about 5 μm (0.25 eV), covering all the visible and near infrared spectral regions. This provides a wide spectral window for photonic applications.

By far, the largest numbers of applications in ferroelectric ceramics remain associated with bulk materials, but a trend toward thin and thick films for some of these applications has recently been observed and has been steadily increasing in intensity. The importance of ferroelectrics for cooling has recently got an impetus. Ferroelectrics can be cooled by applying an electric field to them under certain conditions (“*electrocaloric effect*”). Recently, Mischenko et al. measured  $\Delta T = 12$  K at 25 V across 350 nm of PZT film, which is sufficient to design a prototype cooler for computer mainframes.

The fact that ferroelectrics emit copious electrons (*electron emitter*) from their surfaces during switching has been known for many years. First discovered in Michigan by Rosenblum, this phenomenon was later investigated extensively at Centre European pour la Recherché Nucleaire (CERN) and in France, Poland, Israel, and the United States. Currents of tens of amperes have been obtained with synchronized, monoenergetic pulse lengths of 100 ns to 1 μ these are superior to thermionic cathodes in that the ferroelectrics have higher current densities and lifetimes and also have instant turn-on (thermionic cathodes require a warm-up) capability. This is an unexploited area for which commercial development of miniature high-power microwave devices could be made within a few years.

A *ferroelectric DRAM (FeDRAM)* film, because of its much higher dielectric constant, occupies much less wafer area than the normal SiO<sub>2</sub> capacitor, thus allowing much greater capacity memories to be fabricated on a given silicon wafer. Ferroelectric memories are also nonvolatile. As memories become denser in the future, the transition to ferroelectric films will become a necessity, and operating voltages for these memories will continue to decrease toward 1 V. At present, (Ba,Sr)TiO<sub>3</sub> (BST) film capacitors are the top contenders for these applications. The development of ferroelectric random access memory (*FeRAM*) films for nonvolatile memory applications, such as computer random-access memories, smart cards, and radio-frequency identification tags, is presently underway and has reached modest production levels for specific niche applications [36]. FeRAM films of several compositions, including PZT, PLZT, and SrBi<sub>2</sub>Ta<sub>2</sub>O<sub>7</sub> (SBT), are actively being investigated. Among these, SBT is, perhaps the material of choice in regard to switching fatigue. SBT materials, exhibiting little (<10%) fatigue up to 10<sup>12</sup> switching cycles, have been developed; however,



this value must be increased to  $\sim 10^{14}$  cycles before these films can be used in large-scale applications. Thin-film ferroelectrics exhibit a large decrease in dielectric constant with application of modest voltages. This suggested that they could be used as the active *phase-shift elements* in phased-array radar. Unfortunately, the dielectric loss tangent in these films remains too large for acceptable insertion losses in such devices.

## CHAPTER-2

### MOTIVATION

- ✓ Rare earth oxides are widely used as doping materials for BaTiO<sub>3</sub> ceramics in order to achieve a high dielectric performance and low dissipation factor of the capacitors.
- ✓ The incorporation of trivalent rare-earth cations such in the perovskite lattice of BaTiO<sub>3</sub>, modifies the micro structural and electrical properties of doped BaTiO<sub>3</sub>. The larger ionic size rare-earth ions (La) predominantly dissolve in A-sites, and act as donors, and the intermediate ionic size rare-earth ions, depending on their concentration, dissolve in both A and B- cationic lattice sites in BaTiO<sub>3</sub> structure, and may act as donors or/and acceptors.
- ✓ The substitution of rare-earth ions on Ba<sup>2+</sup> sites requires the formation of negatively charged defects. There are three possible compensation mechanisms: barium vacancies (VBa<sup>''</sup>), titanium vacancies (VTi<sup>'''</sup>) and electrons (e<sup>'</sup>).
- ✓ For samples sintered in air atmosphere, which are electrical insulators, the principal doping mechanism is the ionic compensation mechanism. So in my work I have doped the Ba site of BaTiO<sub>3</sub> perovskite with La to study its effect

## **CHAPTER-3**

### **THESIS OBJECTIVE**

- ✓ To synthesis the high dielectric constant material ( $\text{BaTiO}_3$ ) by sol gel route.
- ✓ To characterize the synthesized materials like XRD for phase formation, SEM for surface morphology and Electrical study for dielectric constant and transition temperature.

## **CHAPTER-4**

### **EXPERIMENTAL TECHNIQUE**

A basic introduction about the experiment use in synthesized and characterized the  $\text{Ba}_{1-x}\text{La}_x/3\text{TiO}_3$  ceramic compound.

#### **4.1. Synthesis methods:**

##### **Calcination**

Calcination is a process of heating, without fusion, to change the physical or chemical constitution of substances. Calcining process consists of 3 main objectives. The first objective is to remove water which is absorbed as water of crystallization or water of constitution. The second objective of calcining is to remove  $\text{CO}_2$ ,  $\text{SO}_2$  and other volatile substances. The third objective of calcination is the oxidation of the substance completely or partially. Calcination is also done in the processes of firing, roasting and burning. Calcination is also referred as calcining. Chemically calcination can be defined as thermal decomposition process applied to substances and ores to bring about phase transition, removal of volatile fractions and thermal decomposition. Calcining process is done on the temperature below the boiling point of the substance subjected to calcinations.

##### **Sintering**

When thermal energy is apply to powder compact, the compact is densified and the average grain size is increases, this process is called sintering and the basic phenomena occurring form this process is densification and grain growth. This is process used to produced density control materials or compound from metal or ceramic powder by applying thermal energy. Sintering aims to produce sintered part with reproducible and if possible designed a microstructure through control the sintering variables.

Microstructural control means control of gain size, sintered density, and size and distribution of other phases including pores. In most of the cases microstructural control prepare a full dense body with fine grain structure.

## Characterization:

The structure provides a variety of concepts, which describes on various scales; its mechanical, chemical or electrical may depends strongly on its internal structure. An understanding of the structure of the material has become essential in the worked of novel materials. A wide range of experimental methods are available for the evaluation of structure of material with high accuracy and precision. The structure and morphology studies are performed by using various techniques such as X-ray diffraction analysis (XRD) and scanning electron microscopy (SEM). The electrical measurement can be done through HIOKI LCR meter in different temperatures.

### XRD analysis

X-ray powder diffraction (XRD) is a rapid analytical technique primarily used for phase identification of a crystalline material and can provide information on unit cell dimensions. The analysed material is finely ground, homogenized, and average bulk composition is determined.

X-ray powder diffraction is most widely used for the identification of unknown crystalline materials (e.g. minerals, inorganic compounds). Determination of unknown solids is critical to studies in geology, environmental science, material science, engineering and biology.

Other applications include

- characterization of crystalline materials
- identification of fine-grained minerals such as clays and mixed layer clays that are difficult to determine optically
- determination of unit cell dimensions
- measurement of sample purity

It is often possible to separate the effects of size and strain. Where size broadening is independent of  $q$  ( $K=1/d$ ), strain broadening increases with increasing  $q$ -values. In most

cases there will be both size and strain broadening. It is possible to separate these by combining the two equations in what is known as the Hall-Williamson method:

$$B.\cos\theta = (k\lambda/L) + \eta.\sin\theta$$

Thus, when we plot  $B.\cos(\theta)$  vs.  $\sin(\theta)$  we get a straight line with slope  $\eta$  and intercept  $k\lambda/L$ .

The expression is a combination of the Scherrer Equation for size broadening and the Stokes and Wilson expression for strain broadening. The value of  $\eta$  is the lattice strain and the value of  $L$  represents the size of the crystalline. The value of constant  $k$  is taken as 0.9.

### **Scanning Electron Microscope (SEM):**

A **scanning electron microscope (SEM)** is a type of electron microscope that images a sample by scanning it with a high-energy beam of electrons in a raster scan pattern. The electrons interact with the atoms that make up the sample producing signals that contain information about the sample's surface topography, composition, and other properties such as electrical conductivity.

All samples must also be of an appropriate size to fit in the specimen chamber and are generally mounted rigidly on a specimen holder called a specimen stub. Several models of SEM can examine any part of a 6-inch (15 cm) semiconductor wafer, and some can tilt an object of that size to 45°. Back scattered electron imaging, quantitative X-ray analysis, and X-ray mapping of geological specimens and metals requires that the surfaces be ground and polished.

### **Dielectric:**

**Dielectric**, insulating material or a very poor conductor of electric current. When dielectrics are placed in an electric field, practically no current flows in them because, unlike metals, they have no loosely bound, or free, electrons that may drift through the material. Instead, electric polarization occurs. The positive charges within the dielectric are displaced minutely in the direction of the electric field, and the negative charges are displaced

minutely in the direction opposite to the electric field. This slight separation of charge, or polarization, reduces the electric field within the dielectric.

The presence of dielectric material affects other electrical phenomena. The force between two electric charges in a dielectric medium is less than it would be in a vacuum, while the quantity of energy stored in an electric field per unit volume of a dielectric medium is greater. The capacitance of a capacitor filled with a dielectric is greater than it would be in a vacuum. The effects of the dielectric on electrical phenomena are described on a large, or macroscopic scale by employing such concepts as dielectric constant, permittivity and polarization.

#### **DSC and TG analysis:**

The DSC and TG analysis of all the three samples is carried out using differential scanning calorimetric and thermo gravimetric analysis (DSC-TG) by heating the sample at 10 °C/min in argon in a thermal analyser (Netzsch, Germany). We take heat flow and mass loss in Y – axis and temperature in X – axis respectively. In DSC, the heat flow increases with increase in temperature.

## **4.2. Experimental work:**

The La doped BaTiO<sub>3</sub> ceramic were prepare by solid state reaction method by taking three raw materials such as (i)Barium acetate( $Ba(CH_3COO)_2$ )(ii) Acetic acid( $CH_3COOH$ ) (iii)Lanthanum acetate( $C_6H_9O_6La$ ) (iv)Titanium isopropoxide( $Ti\{OCH(CH_3)_2\}_4$ ) (v)2-methoxy ethanol solution( $C_3H_8O_2$ ).

- *First, I had mixed barium acetate in acetic acid. After that, I mixed lanthanum acetate and spinning this solution for half an hour.*
- *In another beaker, I took titanium isopropoxide and dissolved in 2-methoxy ethanol solution and spinning this for few minutes.*
- *After this, I added the solution and heating it up to 70oc as well as spinning this one for 3 hrs. and lastly we got powdered form.*
- *We calcined the sample 1000°C per 2 hrs. Then I made pellets and sintered at 1250°C for 20minutes.*

- ceramics were prepared by sol gel route in different values of  $x$  (i.e.,  $x = 0, 0.01, 0.025, 0.05, 0.075, 0.1$ ) in  $Ba_{(1-x)}La_{2x/3}TiO_3$
- For making pellets used binder i.e., poly vinyl alcohol (PVA) solution mix with powder and to make pellets by using hydraulic pressure, to applying around 5 ton pressure for 3 minutes.
- To know the phase formation of prepare (calcinations) sample used XRD analysis technique. Use SEM for surface morphology and EDX for chemical composition of  $Ba_{1-x}La_{2x/3}TiO_3$  ceramic compound and at last measured the electrical properties i.e., dielectric and curie constant.

### FLOWCHART:

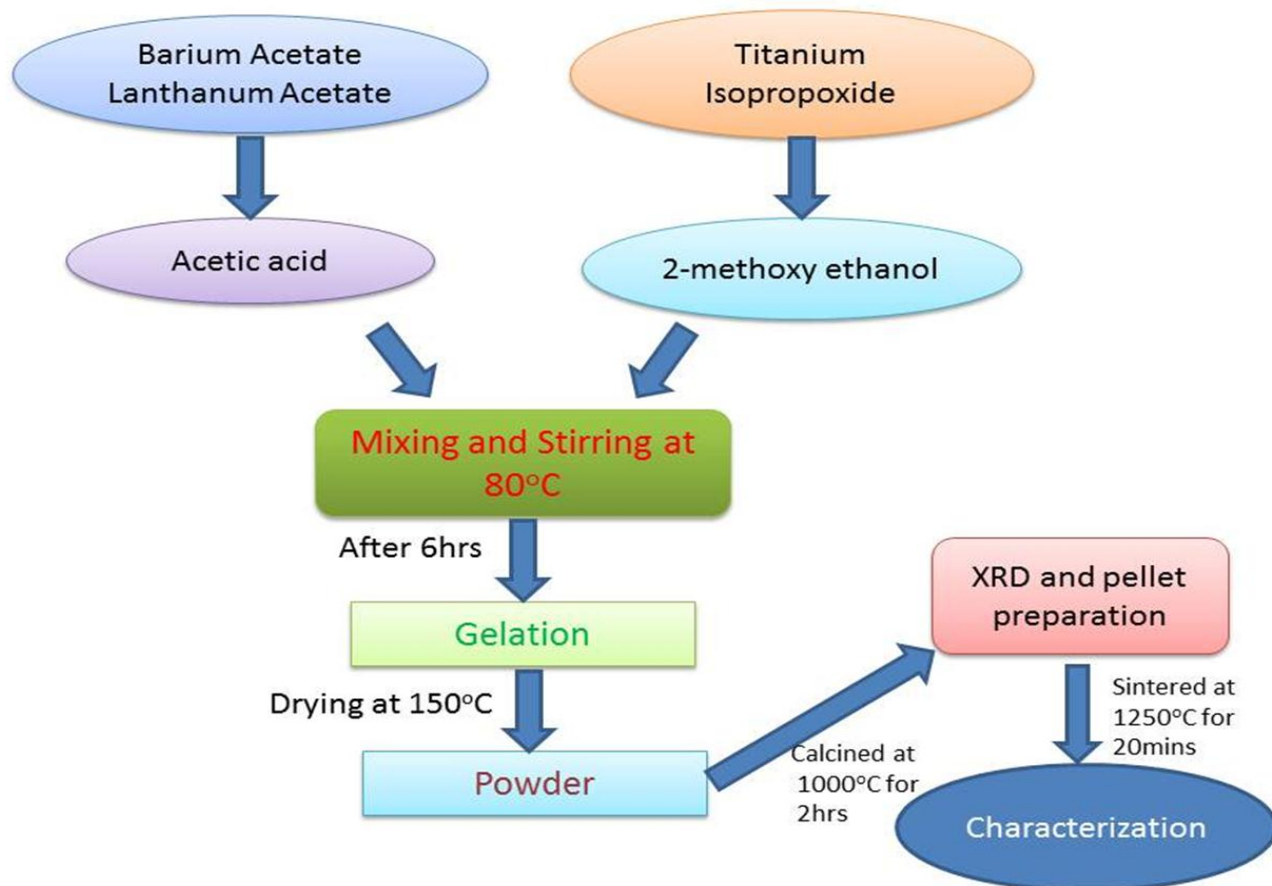


**Fig.6. Flow chart of experimental work**



## CHAPTER-5

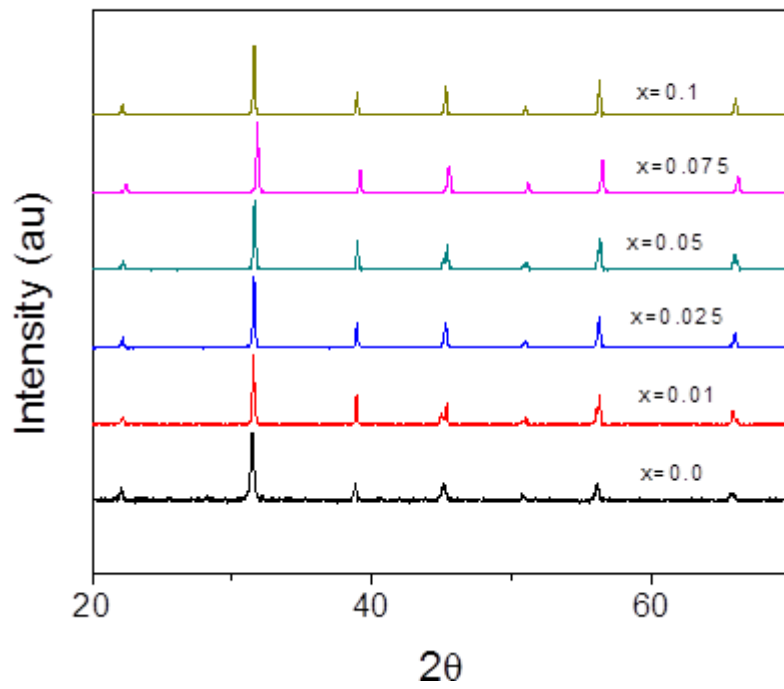
### RESULTS AND DISCUSSION

#### 5.1 XRD Analysis:

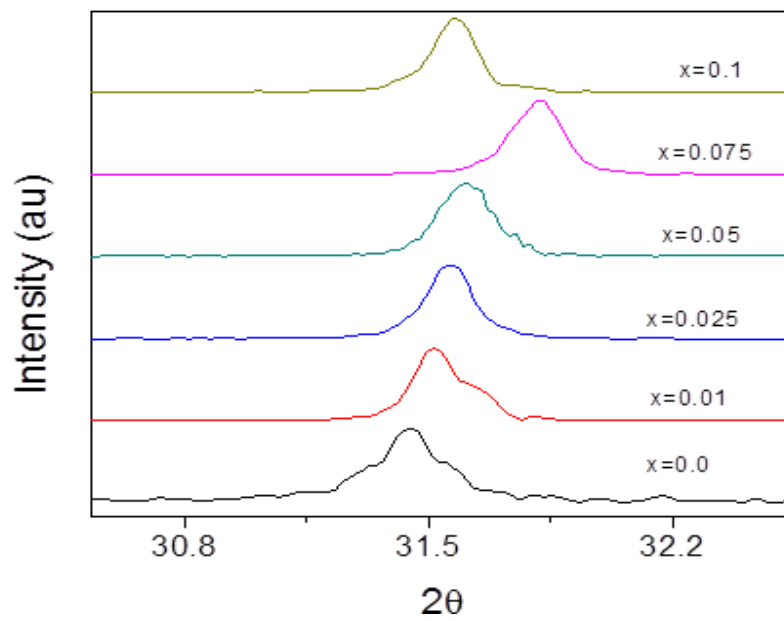
The  $\text{Ba}_{1-x}\text{La}_{2x/3}\text{TiO}_3$  ceramics were prepared by solid state reaction route. The synthesized powders were characterized by X-ray diffraction using a PANALYTIC diffractometer. XRD pattern were obtained using  $\text{Cu K}\alpha$  radiation and the Fig.7.shows the XRD pattern of the La doped  $\text{BaTiO}_3$  range from 20-70o in  $2\theta$  scale at the rate of  $0.04^\circ/\text{second}$ . According to JCPDS no.05-0626, all the peaks in the patterns are matching and its showing purely tetragonal single phase crystal related to tetragonal  $\text{BaTiO}_3$ . The crystal single phase crystals of the  $\text{Ba}_{1-x}\text{La}_{2x/3}\text{TiO}_3$  ceramics are tetragonal symmetry in the space group  $P4\text{mm}$ . No evidence of the precursor phase  $\text{BaCO}_3$ ,  $\text{TiO}_2$  or  $\text{Bi}_2\text{O}_3$  was detected by XRD and all the matched  $hkl$  values are indexed in the Fig.7. From Fig.7, it is well known that the tetragonal phase was identified by an analysis of the peaks [002] and [200] at the  $2\theta$  from 44.5-46. Table-1 shows the parameters about the peak position, FWHM, a, b, c parameters, volume, c/a. The peak shifts toward right indication a decrease in lattice parameter.

**Table-1**

compositions	FWHM	$2\theta$ positions	a	b	c	volume
X=0.01	0.1200	31.5097	3.9961	3.9961	4.0294	64.34
X=0.025	0.1680	31.5688	4.0020	4.0020	4.0060	64.16
X=0.05	0.1920	31.6239	3.9945	3.9945	4.0163	64.08
X=0.075	0.1680	31.8329	3.9876	3.9876	3.9748	63.20
X=0.1	0.1920	22.1841	4.0029	4.0029	3.9996	64.09



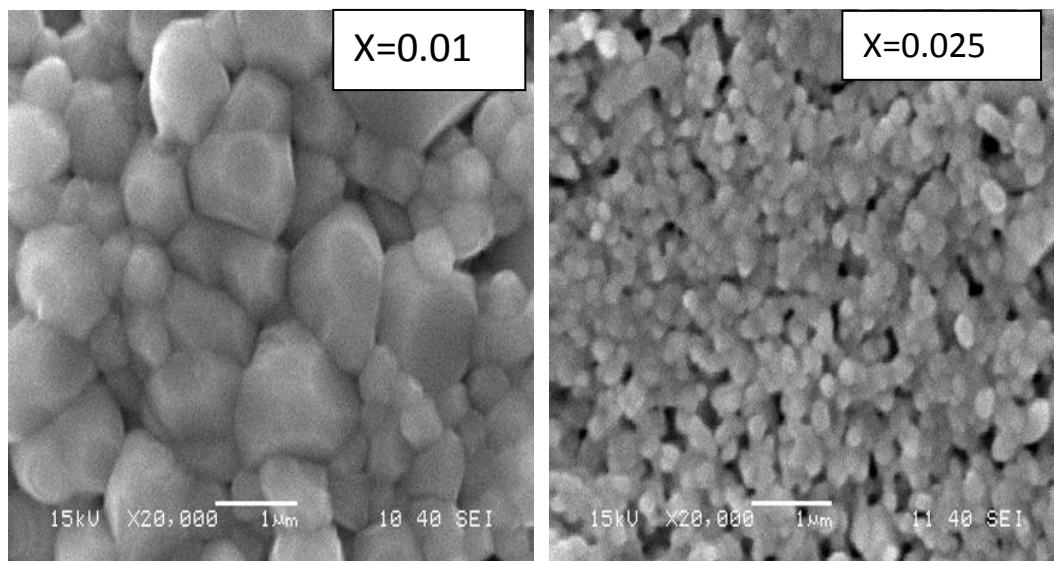
**Fig.7. XRD patterns Of all samples**



**Fig.8. XRD pattern**

## 5.2 SEM Analysis:

Microstructural features were studied using Scanning Electron Microscope (JSM 6480 LV JEOL, Japan). The SEM microstructure of all samples is given in figure 7. All the samples are leached and sintered. Fig.8. shows the SEM of sintered samples at 1250<sup>0</sup>C. Another important thing one may observe while comparing the micrographs of the sintered samples that the grain size goes on decreasing as we increase doping concentration  $x=0.01$  to 0.05, the grain size is decreasing. At the concentration of  $x=0.01$ , it is seen that the grain size is neatly grown. At  $x=0.1$  and 0.075 the grains are shown to be melted and agglomerated.



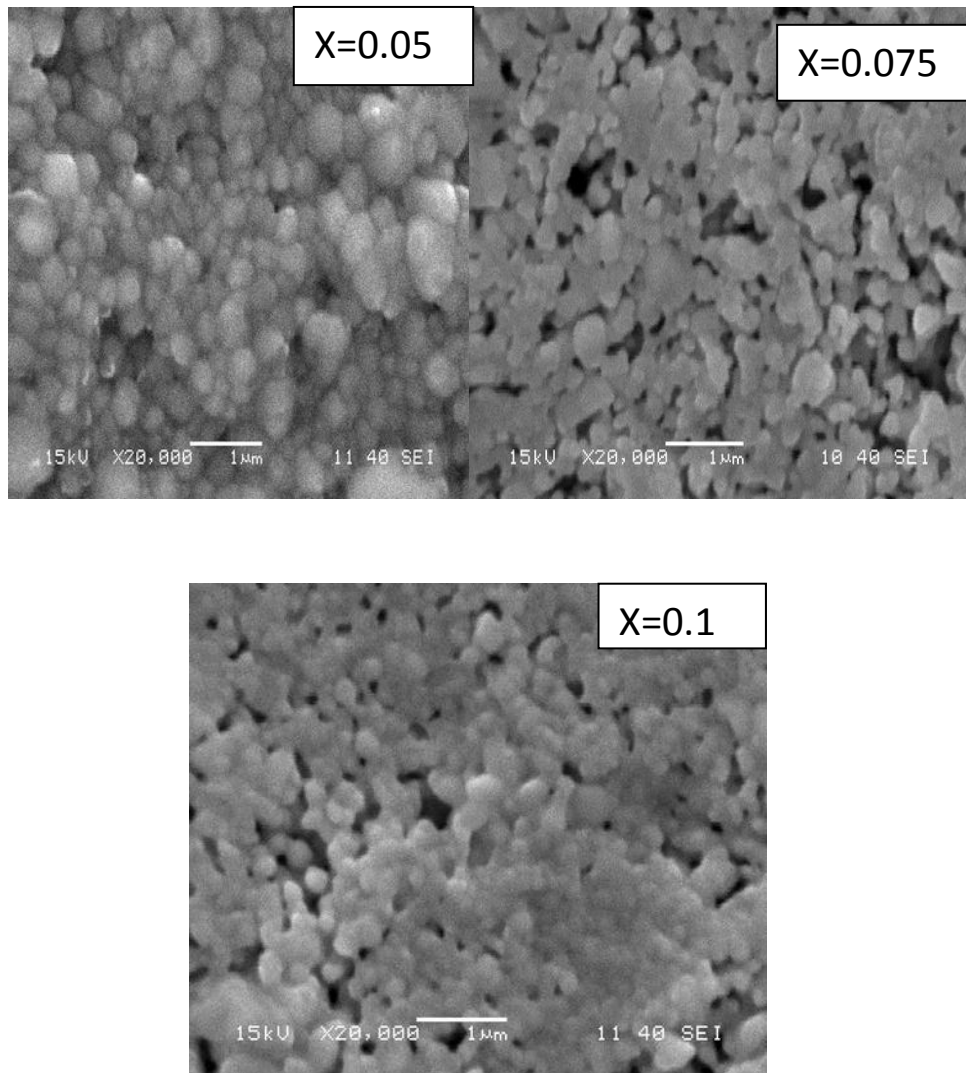


(**Fig.9.** SEM picture of Ba<sub>1-x</sub>La<sub>2x/3</sub>TiO<sub>3</sub> pellets for all composition of x)

### 5.3 DSC and TG analysis:

The DSC and TG analysis of all the three samples is carried out using differential scanning calorimetric and thermo gravimetric analysis (DSC-TG) by heating the sample at 10 °C/min in argon in a thermal analyzer (Netzsch, Germany). The plots are shown in the figure 6(a), 6(b) & 6(c). Figure 6(a) shows the DSC and TG analysis of unleached & calcined BFO, by taking heat flow and mass loss in Y – axis and temperature in X – axis. In DSC, the heat flow increases with increase in temperature. Sharp endothermic peaks at 99°C, 333°C, 764°C are observed. The TG plot of BFO reveals a broader decrease in mass near 1000°C due to evaporation of water molecules. As we gradually increase the temperature there is a considerable loss of mass around 250-450°C, which is a broader one.

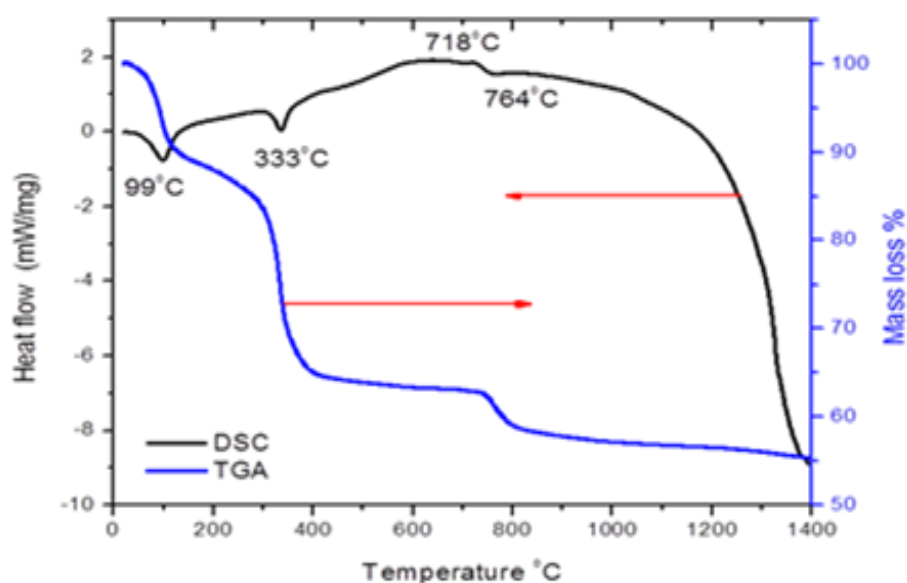


**Fig.10.** DSC and TG plot of calcined BaTiO<sub>3</sub>

## 5.4 Dielectric:

In Fig.10 shows the Relative permittivity of sintered pellets of  $Ba_{1-x}La_{2x/3}TiO_3$  for  $x= 0, 0.025$  and  $0.05$ . The sintered samples were coated with silver paste on both sides and heated at  $500^\circ\text{C}$  for 30 minutes for perfect conductivity of the electrodes.

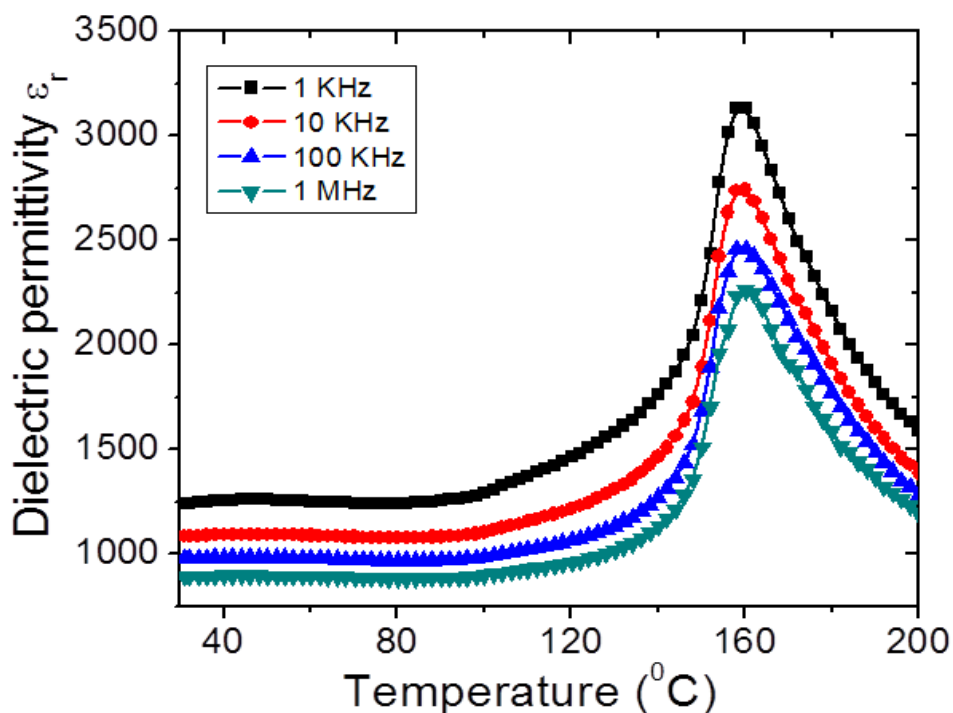


**Fig.11.** Relative permittivity Vs. Temperature of sintered pellets of BT.

In most ferroelectrics, the temperature dependence of the relative permittivity above the Curie temperature (in paraelectric phase regime) can be described accurately by a simple relationship called the Curie-Weiss law.

$$\epsilon = \epsilon_0 + \frac{C}{T - T_0}$$

Where,  $C$  is the Curie-Weiss constant and  $T_0$  the Curie- Weiss temperature. Generally, in the case of a first-order phase transition,  $T_0 < T_c$ , while for the second-order phase transition  $T_0 = T_c$ . Fig.19 shows the variation of inverse relative permittivity with temperature in the vicinity of transition temperature for  $\text{Ba}_{1-x}\text{La}_{2x/3}\text{TiO}_3$  ceramics sintered at  $1300^\circ\text{C}$ . The dielectric data show clearly first-order phase transition and excellent Curie-Weiss behaviour. The Curie constant ( $C$ ) obtained for this sample composition  $x = 0.0$ .

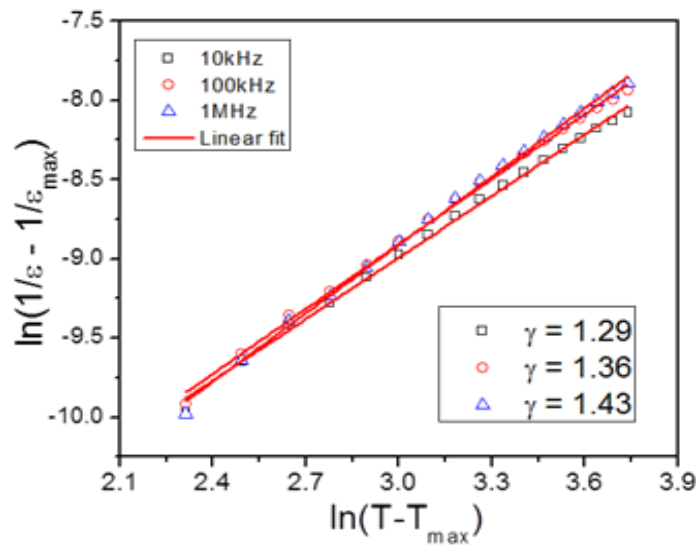


**Fig. 12.** (Colour online) The  $\log (1/\epsilon - 1/\epsilon_{\max})$  vs.  $\log (T - T_{\max})$  plot of BT Ceramics at a measurement frequency of 100 kHz.

## 5.5 P-E loop measurement:

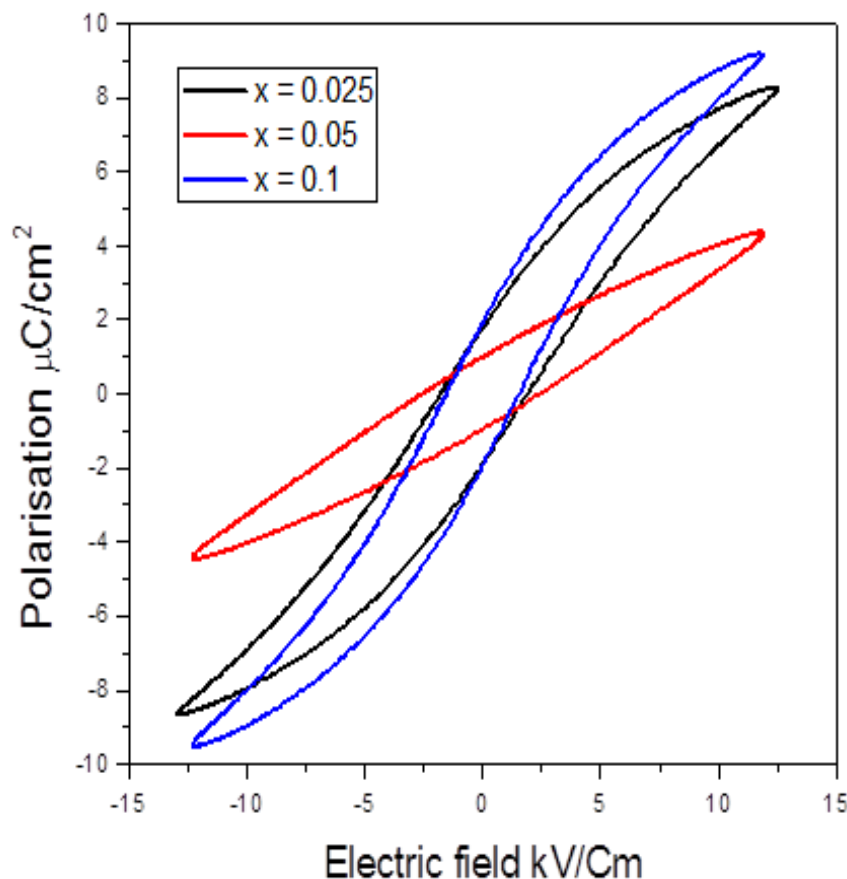


**Fig.13** .Ferroelectric hysteresis loop of  $\text{Ba}_{1-x}\text{La}_{2x/3}\text{TiO}_3$

Fig. 13 shows the ferroelectric hysteresis loop of La doped BaTiO<sub>3</sub> ceramics obtained under a maximum applied electric field of 15 kVcm<sup>-1</sup>. The breakdown of the undoped BaTiO<sub>3</sub> ceramic (at 19kVcm<sup>-1</sup>) is very faster than the doped one. The P–E loop for all the compositions are recorded at room temperature and at a frequency of 100 Hz. The values of remnant polarization (Pr) and coercive field (Ec) are listed in Table-2. For doped samples, the increase in Pr may be due to the decrease in concentration of oxygen vacancies in the system. As a result, the domain pinning effect gets decreased, enhancing Pr.



**Table-2**

Composition	$P_r(\mu\text{C}/\text{cm}^2)$	$E_c(\text{kV}/\text{cm})$	$P_{\text{sat}} (\mu\text{C}/\text{cm}^2)$
X=0.1	1.929	1.534	9.329
X=0.025	1.838	1.846	8.498
X=0.05	0.984	2.504	4.419

Table -1 shows the values of remnant polarisation ( $P_r (\mu\text{C}/\text{cm}^2)$ ), coercive field  $E_c(\text{kV}/\text{cm})$  and saturation polarisation of  $\text{Ba}_{1-x}\text{La}_{2x/3}\text{TiO}_3$  ceramic of compositions X=0.1, X=0.025 and x=0.05 respectively.

## CHAPTER-6

### CONCLUSIONS

- From XRD graph it is seen that the peak is shifting towards right due to doping of La on A site on BT ceramic.
- SEM shows at doping concentrations  $x=0.01$  to  $0.05$  the grain size is decreasing. At the concentration of  $x=0.01$  it is seen that the grain size is neatly grown. At  $x=0.1$  and  $0.075$  the grains are shown to be melted and agglomerated.
- From the DSC-TGA graph, it is seen that the organic materials are getting removed at the time of endothermic reaction and getting crystallized at the time of exothermic reaction.
- From the dielectric study, we can calculate  $\gamma$ , the diffusivity factor. Here  $\gamma$  ranges between  $1.29$  to  $1.43$ . So it shows diffusive nature but still it is a normal ferroelectric.

## REFERENCES

1. Henning D, Schnell A, and Simon G, *J Am. Ceram Soc*, 65 (1982) 539-544.
2. Yu Z, Guo R , Bhalla A S, *J.appl. Phys*, 88 (2000) 410.
3. Yu Z, Ang C, Guo R, Bhalla A S, *Appl. Phys. Lett*, 81 (2002) 1285.
4. Sciau Ph, Calvarin G, Ravez *J Solis State Communications*, 113 (2000) 77-82.
5. Wu T B, Wu C M and Chen M L, *Appl Phys Lett*, 69 (18) (1996) 2659,
6. Abe K, and Komatsu S, *J.appl. Phys*, 77 (1995) 6461.
7. Lu S G, Zhu X H, Mak C L, Wong K H, Chan H L W, and Choy C L, *Appl Phys Lett*. 82 (2003) 2877.
8. Zhu X H, Chong N, Lai-Wah Chan H, Mak C L, Wong K H, Liu Z G, and Ming N B, *Appl Phys Lett* 80 (2002) 3376.
9. Wang C, Cheng B L, wang S Y, Lu H B, Zhou Y L, Chen Z H, Yang G Z, *Appl Phys Lett*, 84 (5) (2004) 765.
10. “Elements of x-ray diffraction” Cullity B D, 2nd Edition, Addison- Wesley Publishing company, Inc.
11. Wong T K Y, Kennedy B J, Howard C J, Hunter B A, Vogt T , *J Solid State Chemistry*, **156**, 255 (2001).

12. Astala R K and Bristowe P D, *Modelling Simul. Mater. Sci Eng* **12** (2004) 79-90.
13. R. Pepinsky, Y. Okaya and F. Unterleitner, *Acta. Cryst.*, **13**, 1071 (1960).
14. L. E. Cross, *Ferroelectrics*, **76**, 241 (1987).
15. N. Vittayakorn et. al. "Dielectric Properties of Bismuth Doped Barium Titanate (BaTiO<sub>3</sub>) Ceramics" *Journal of Applied Science Research* **12** 1319 (2006).
16. M. R. Panigrahi et. al. "Synthesis and microstructure of Ca-doped BaTiO<sub>3</sub> ceramics prepared by high-energy ball-milling", *Physica B*. **404**, 4267 (2009).
17. M. R. Panigrahi et. al. "Structural analysis of 100% relative intense peak of Ba<sub>1-x</sub>Ca<sub>x</sub>TiO<sub>3</sub> ceramics by X-ray powder diffraction method", *Physics B*. **405**, 1787 (2010).
18. Andrew J. Bell et. al. "Ferroelectrics: The role of ceramic science and engineering", *Journal of the European Ceramic Society*. **28**, 1307 (2008).
19. S. ZHANG et. al. "Normal ferroelectric to ferroelectric relaxor conversion in fluorinated polymers and the relaxor dynamics", *J. Materials Science*. **41**, 271 (2006).
20. N. Abdelmoula et. al. "Relaxor or classical ferroelectric behavior in A-site substituted perovskite type Ba<sub>1-x</sub>(Sm<sub>0.5</sub>Na<sub>0.5</sub>)<sub>x</sub>TiO<sub>3</sub>", *Solid State Sciences*. **8**, 880 (2006).

